Behavior of oxidized platinum nanoparticles on an aligned carbon nanotube forest

Keita Matsuda' , Wataru Norimatsu, Shigeo Arai, and Michiko Kusunoki

Citation: J. Appl. Phys. **120**, 142111 (2016); doi: 10.1063/1.4961721
View online: http://dx.doi.org/10.1063/1.4961721
View Table of Contents: http://aip.scitation.org/toc/jap/120/14
Published by the American Institute of Physics

Behavior of oxidized platinum nanoparticles on an aligned carbon nanotube forest

Keita Matsuda,[1,a)] Wataru Norimatsu,[1] Shigeo Arai,[2] and Michiko Kusunoki[2]
[1]*Department of Applied Chemistry, Nagoya University, Nagoya 464-8603, Japan*
[2]*Institute of Materials and Systems for Sustainability, Nagoya University, Nagoya 464-8603, Japan*

(Received 29 April 2016; accepted 4 August 2016; published online 30 August 2016)

We observed and analyzed the behavior of platinum nanoparticles (PtNPs) supported on aligned-carbon nanotubes (CNTs) at high temperatures by X-ray photoelectron spectroscopy and high-resolution transmission electron microscope observations. We found that the PtNPs moved toward the inner-side along each CNT on which they were deposited. The mechanism of this behavior is related to the redox reaction of Pt with the carbon atoms in the CNT. We also performed *in-situ* observation of this process at a high temperature using an environmental transmission electron microscope under an oxygen atmosphere. We found that the PtNPs penetrated down into a high-density aligned CNT forest along the tube axis and that the PtNPs changed their shape to fit the structure of the CNTs during their movement. *Published by AIP Publishing.*
[http://dx.doi.org/10.1063/1.4961721]

I. INTRODUCTION

Carbon nanotubes (CNTs) have attracted great attention since their discovery.[1] We have previously reported that the well-aligned CNT films were formed on silicon carbide (SiC) by SiC surface decomposition. The CNT films formed by this method are well-aligned, highly dense, and maintain direct bonds with the SiC surface atoms.[2–4]

It is generally known that the best catalysts for some kinds of fuel cells are platinum (Pt) or its alloys, but they are rare and expensive.[5,6] Many researchers then have investigated effective Pt loading methods.[7–9] One of the effective Pt loading methods is the application of carbon material as a support for Pt catalysts.[10] In particular, CNTs are interesting candidates for supporting materials because of their superior characteristics such as a high specific surface, and high electrical and thermal conductivities.[11,12] In order to apply CNTs as such supports, investigations into the mechanism of deterioration of Pt and its supporting materials at elevated temperatures have been required.[13] Recently, we found a phenomenon that Pt deposited on CNT films etched the CNTs at 500 °C or higher temperatures in air.[14] In the present study, in order to clarify this phenomenon involving Pt under such conditions, we investigated the change of the surface chemical state of the deposited platinum nanoparticles (PtNPs) by X-ray photoelectron spectroscopy (XPS) and carried out *in-situ* observation of Pt nanoparticles (PtNPs) with an environmental transmission electron microscope (E-TEM) at elevated temperatures.

II. EXPERIMENTAL PROCEDURES

A. Surface characterization

The aligned CNT films with a thickness of 200 nm were prepared by holding 6H-SiC $(000\bar{1})$ substrates at 1600 °C for 1 h in a vacuum of 1×10^{-2} Pa. The PtNPs were deposited on the CNT films under the conditions of the sputtering pressures of ~8 Pa, a sputtering current of 10 mA, and a duration of 12 s by a magnetron sputtering apparatus. We prepared two samples with different degrees of oxidation of Pt. We hereafter call the highly and poorly oxidized samples as samples 1 and 2, respectively. We also prepared sample 3 by annealing sample 1 at 500 °C for 5 min in a vacuum of 1×10^{-2} Pa to remove surface oxides from the PtNPs. These three Pt-deposited CNT films were then heated at 525 °C for 30 min with a mixed gas of oxygen and nitrogen with the ratio of O_2:N_2 = 1:4. The chemical bonding state of the PtNPs on the CNT films before and after the heat treatment was investigated by XPS measurements with an ESCA-3300 instrument using Mg Ka radiation as the X-ray source. Landscapes of the PtNPs deposited on the CNTs before and after the heat treatment were observed by an EM-002B-type transmission electron microscope at an accelerating voltage of 200 kV.

B. *In-situ* TEM observation

We carried out *in-situ* TEM observations of the PtNPs' behavior at elevated temperatures. For heating the sample, we used a tungsten spiral wire, on which the powder samples needed to be supported. The powder samples were prepared by the following procedure.

First, we heated 3C-SiC powder (IBIDEN CO., Ltd.) with an average diameter of 300 nm to 1700 °C and held at that temperature for 3 h in an Ar gas atmosphere at 3 atm pressure in the electric furnace, in order to smoothen their surface. The reason we used 3C-SiC was that we can only purchase 3C-SiC in the powder form. The diameter of the SiC particles was increased by the first heating. Second, we heated the resulting round-shaped 3C-SiC particles now with an average diameter of about 1 μm to 1700 °C and held them at that temperature for 2 h in a vacuum of 1.0×10^{-2} Pa to grow CNTs. We thus obtained radially aligned CNTs (aggregated CNTs

This paper is part of the Special Topic "Cutting Edge Physics in Functional Materials" published in J. Appl. Phys. **120**, 14 (2016).
a)Electronic mail: matsuda.keita@c.mbox.nagoya-u.ac.jp

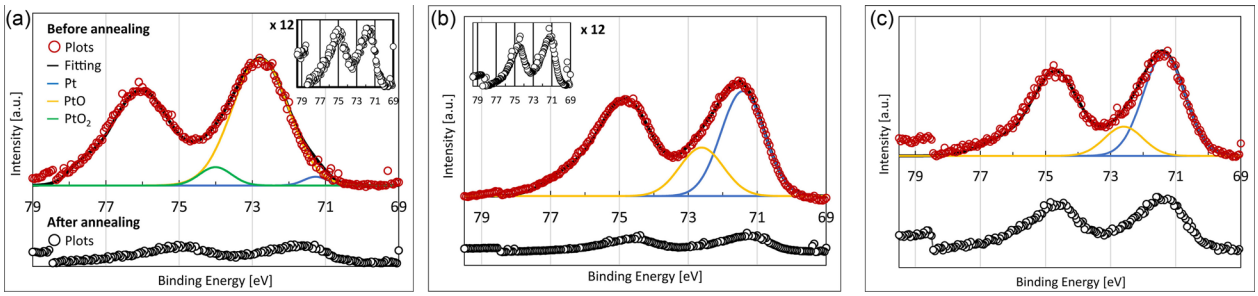

FIG. 1. XPS results of Pt 4f 7/2 spectra obtained from (a) sample 1, (b) sample 2, and (c) sample 3. XPS spectra obtained before the heat treatment were shown in the upper sections and those obtained after the heat treatment were in the lower sections (Inset: enlarged spectra of the lower one). The positions and ratios of each peak were listed in Table I.

particle) with a small amount of 3C-SiC remaining in its center. The PtNPs were deposited on the aggregated CNTs particle by magnetron sputtering under the pressure (8 Pa) and the current (10 mA), which is the same condition as in the sample 1, but the duration was 10 times longer (120 s) than the sample 1 to obtain larger PtNPs in order to easily find the PtNPs in the limited resolution of the *in-situ* observation. The Pt-deposited CNT particles were placed in ethanol and were dispersed on the tungsten spiral wire used as an electrical resistance heater which itself was attached to an environmental ultra-high voltage (E-UHV) TEM sample holder. *In-situ* observation by an E-UHV TEM was carried out using a JEM-1000 K RS-TEM (JEOL, Ltd.) at an accelerating voltage of 1000 kV. A calibration curve of temperature vs. current was obtained from the melting point and decomposition temperature of aluminum (670 °C), copper (1040 °C), and Al_2O_3 (1350 °C). The samples were heated to about 800 °C under 1.8×10^{-4} Pa of oxygen pressure in the E-UHV TEM. Oxygen gas was blown onto the samples from a nozzle with an inside diameter of 0.5 mm φ introduced into the E-UHV TEM.[15]

III. RESULTS

A. Change in the PtNPs deposited on the CNT film

The XPS spectra from the Pt 4f orbital obtained from each Pt-deposited CNT film are presented in Fig. 1. In each figure, the spectra before and after the heat treatment are shown in the upper and lower panel. Before the heat treatment, the spectrum of sample 1 could be fitted by three components. On the contrary, the spectra of samples 2 and 3 could be fitted by just two components. The binding energies for the Pt 4f 7/2 peaks were found to be around 71.3, 72.8, and 74.0 eV in sample 1; 71.4 and 72.6 eV in sample 2; and 71.4 and 72.6 eV in sample 3, respectively. After the heat treatment, those were found to be around 71.6 and 72.8 eV in sample 1; 71.3 and 72.6 eV in sample 2; and 71.4 and 72.5 eV in sample 3, respectively. These values were in good agreement with those reported for Pt (71.3 eV), PtO (72.4 eV), and PtO_2 (74.2 eV).[17] Table I shows peak positions and ratios of the peak areas of three components in the three samples before and after the heat treatment. The peak area ratios were calculated from the area (A) of each Pt 4f 7/2 peak according to the following equation:

$$Peak\ area\ ratio\ [\%] = \frac{A_{Pt,\,PtO,\,or\,PtO_2}}{A_{Pt} + A_{PtO} + A_{PtO_2}} \times 100. \quad (1)$$

The PtNPs of sample 1 mainly consisted of platinum oxides (PtO and PtO_2), and the PtNPs of samples 2 and 3 consisted of several tens % of metallic platinum and a few tens % of PtO before the heat treatment. After the heat treatment, the majority of all samples were metallic platinum, indicating that the oxidized platinum was reduced by the heat treatment. The intensities of Pt 4f peaks of samples 1 and 2 were significantly weak after the heat treatment, which indicates that the platinum was rarely present around the surface of the film. On the other hand, in sample 3, the intensity did not change so much, and the peak positions before and after the heat treatment were also similar. In other words, the metallic platinum seemed not to react with the CNTs by the heat treatment.

In order to understand the situation of the PtNPs after the heat treatment, we performed cross-sectional TEM observations of the Pt-deposited CNT films. Figures 2(a)–2(c) and 2(a)′–2(c)′ show TEM images of the PtNPs on the CNT film formed on the 6 H-SiC substrate before and after the heat

TABLE I. Peak area ratios of binding energy for the Pt 4f 7/2 electron peaks.

	Literature[17]		Sample 1		Sample 2		Sample 3	
			Before	After	Before	After	Before	After
Pt	71.3 eV	Position	71.3 eV	71.6 eV	71.4 eV	71.3 eV	71.4 eV	71.4 eV
		Volume	3%	81%	69%	78%	79%	82%
PtO	72.4 eV	Position	72.8 eV	72.8 eV	72.6 eV	72.6 eV	72.6 eV	72.5 eV
		Volume	89%	19%	31%	22%	21%	18%
PtO2	74.2 eV	Position	74.0 eV	…	…	…	…	…
		Volume	8%	…	…	…	…	…

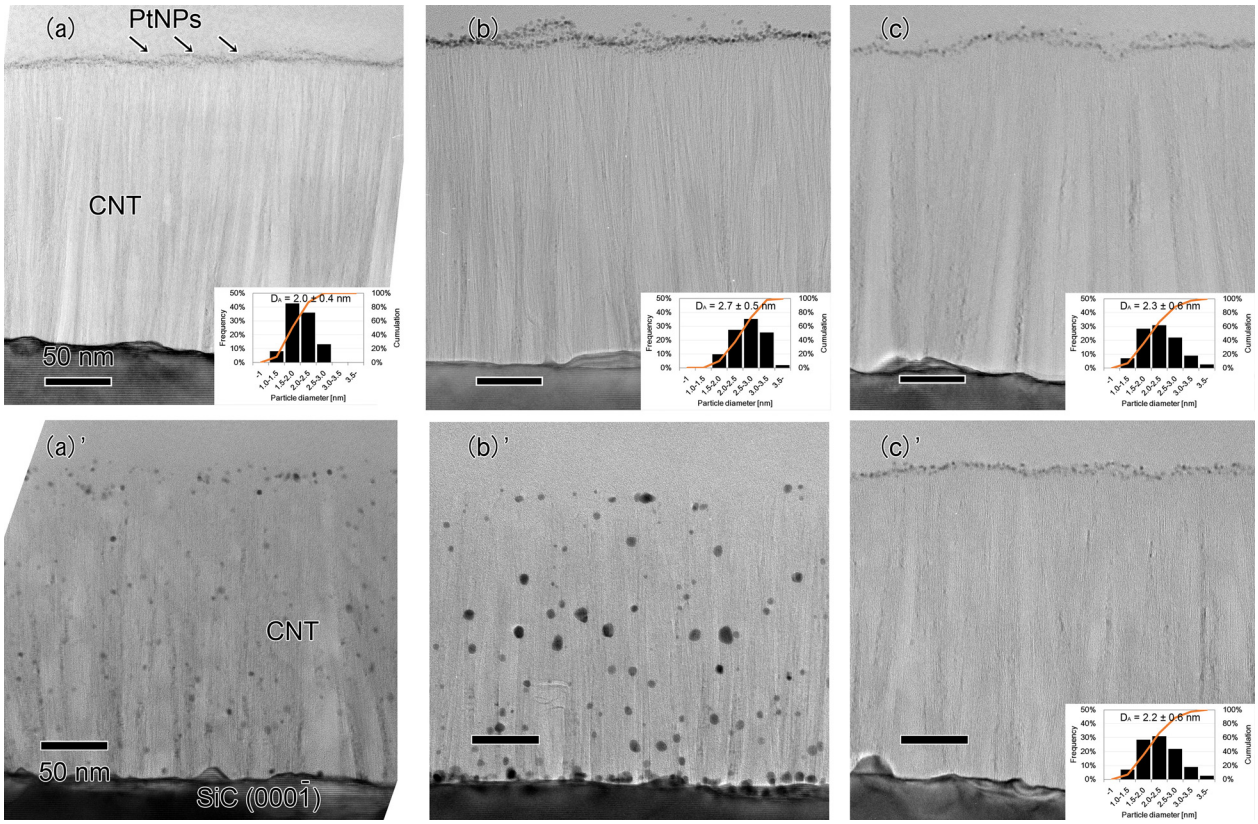

FIG. 2. TEM images of the PtNPs on the CNT films before the heat treatment: (a) sample 1, (b) sample 2, and (c) sample 3. (a)′–(c)′ TEM images of the PtNPs on the CNT films after the heat treatment: (a)′ sample 1, (b)′ sample 2, and (c)′ sample 3. The insets show the size distributions of the deposited PtNPs.

treatment, respectively. The PtNPs with the size of about 2–3 nm were found on the top of the film before the heat treatment. The size distributions are shown in the inset of each TEM image. We found obvious differences between before and after the heat treatment in samples 1 and 2, while there was no significant change in sample 3. The PtNPs in samples 1 and 2 penetrated into the aligned CNT films. In addition, the contrast in the CNT film was partially faint, indicating that some CNTs were partially etched away. Figure 3(a) shows an HR-TEM image of the PtNP in sample 1 after the heat treatment. A clear lattice image can be observed on the edge of the CNT. A fast Fourier transform (FFT) pattern shown in the inset of Fig. 3(a) was obtained from the red square. All diffraction spots were well explained as a diffraction pattern with the electron incidence parallel to the [110] zone axis of Pt. This result as well as XPS analyses indicated that the platinum oxides were reduced to Pt in sample 1. Figures 3(b) and 3(c) show TEM images of the PtNPs in sample 2 after the heat treatment. The PtNPs increased in size up to a few tens of nanometers. Some PtNPs had a lattice spacing of 2.3 Å as shown in Fig. 3(b), which corresponds to the interplanar distance of the (111) plane of Pt. The size of the PtNPs became larger, and they were found along the CNT walls as shown in Fig.

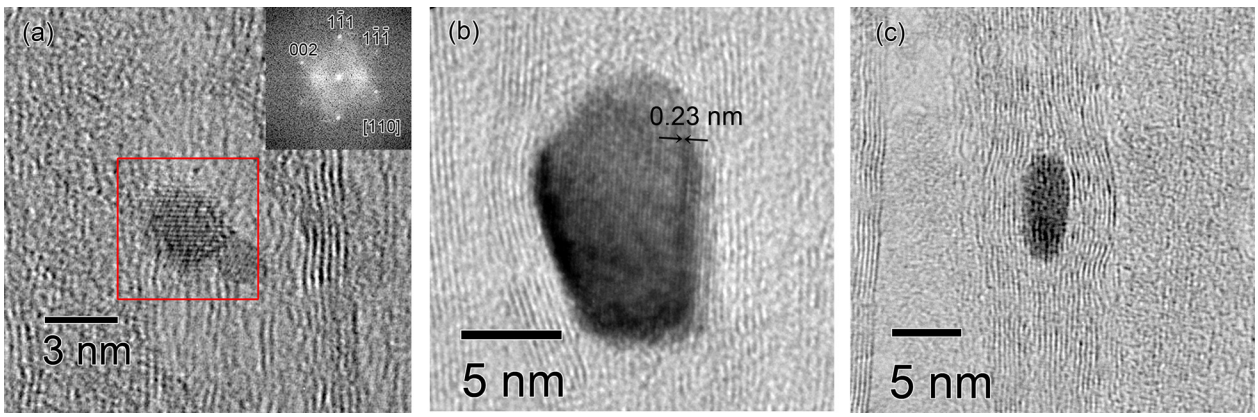

FIG. 3. TEM images of the PtNPs penetrated into the CNT films after the heat treatment in sample 1 (a) and sample 2 (b) and (c). (a) High-resolution TEM image together with the FFT pattern taken from the red square. (b) The typical lattice spacing was confirmed. (Left) CNT walls were pushed out from the inside. (Right) PtNP formed a (111) facet along the wall. (c) PtNP grew at the interlayer of the CNT walls.

3(b). The increased growth of the PtNPs led to a bulging wall that was being pushed out from the inside of the CNT, as shown in Fig. 3(b). Some PtNPs aggregated in or between the CNTs, thereby expanding the walls, as shown in Figs. 3(b) and 3(c). In sample 3, we could not observe any significant change in the PtNPs.

B. *In-situ* TEM observations

Before proceeding to the results of *in-situ* observations, we describe features of the aggregated CNTs particle used for observation. Figure 4(a) shows a whole image of a typical aggregated CNTs particle, whereas Fig. 4(b) shows a magnified image of the CNT caps around the particle. It should be noted again that we need particle-type samples for the *in-situ* high-temperature observations. Radially aligned and highly dense CNTs can be observed with a small amount of residual 3C-SiC inside the CNTs, shown by arrows. This suggests that the CNTs grew perpendicular to the surface of the 3C-SiC particle. The average diameter and length of the CNTs obtained from 3C-SiC were about 4 nm and about 100–300 nm. Those of the CNTs obtained from 6H-SiC were about 4 nm and about 200 nm, indicating the similarity of the features of CNTs on the 3C-SiC particle and on the 6H-SiC single crystal substrate.[18]

We performed *in-situ* TEM observations to capture the dynamic behavior of the PtNPs during penetration into these CNTs. Click Fig. 5 (see supplementary material) to watch the movie file of the *in-situ* TEM observation in the supplementary material. Figures 5(a)–5(d) show snapshots of the movie, showing the behavior of a PtNP with a diameter of 100 nm on an aggregated CNTs particle of about 600 nm. Figure 5(a) is the image at room temperature together with the corresponding schematic image in the inset. Figures 5(b)–5(d) show a series of images during the heat treatment at 817 °C. Before the heat treatment, the PtNP had facets as shown in Fig. 5(a), suggesting the platinum metal. As the temperature increased, it became rounded, which may possibly correspond to the surface oxidation.[16] After being heated for 20 min at 817 °C, the PtNP started to tunnel down into the CNTs along their axis as shown in Figs. 5(b)–5(d). As the PtNP passed through the CNTs, it changed to a slightly brighter contrast, as shown by dotted red lines in Fig. 5(d). This change indicated that the CNTs that were in the way of the PtNP as it passed through were removed. While penetrating the CNTs, the PtNP changed its front shape flexibly, as shown in Figs. 6(a)–6(d). In particular, we noticed that it was branching actively at the interface between the PtNP and the CNTs as if it repeatedly extended and retracted its "tentacles." In Fig. 6(d), we can see a tentacle extended in a longer and slim manner, reflecting the anisotropy of the radially aligned CNTs. These features suggest that the reaction takes place in the interface between the PtNP and the CNT. The PtNP penetrated into the CNTs in the time scale of tens of minutes, while the tentacles extended and retracted in the time scale of tens of seconds.

IV. DISCUSSION

As described in Sec. III, there were significant differences among the three PtNPs after the heat treatment. In samples 1 and 2, the PtNPs penetrated into the CNT films and coalesced after the heat treatment. In addition, in sample 1, although the PtNPs mainly consisted of platinum oxides (PtO and PtO_2) before the heat treatment, we confirmed the existence of metal Pt nanoparticles and the increase in the ratios of metallic platinum after the heat treatment. The similar changes were also observed in sample 2. On the other hand, in sample 3, the initial chemical states and size distribution of the metal PtNP deposited on the top of the CNTs remained even after the heat treatment.

Based on these results, we discuss here the driving force of the movement of PtNPs. The results mentioned above indicate that the existence of the platinum oxides is an important factor for this phenomenon. In other words, a redox reaction between the platinum oxides and the CNTs could be a key step. We presented the equation:

$$2PtO_x + xC(CNT) \rightarrow 2Pt + xCO_2. \quad (2)$$

The standard formation enthalpies of CO_2, PtO, and PtO_2 are −394, −71, and −134 kJ/mol, respectively,[19] indicating the validity of Eq. (2). Figure 7 is a schematic diagram of the reaction between the platinum oxide and the CNTs. The redox reaction first etches the CNT caps and then proceeds to the inner CNTs film. The reaction will last until all the platinum oxides turn into platinum metal. On the other hand, if the PtNPs do not contain a significant amount of the

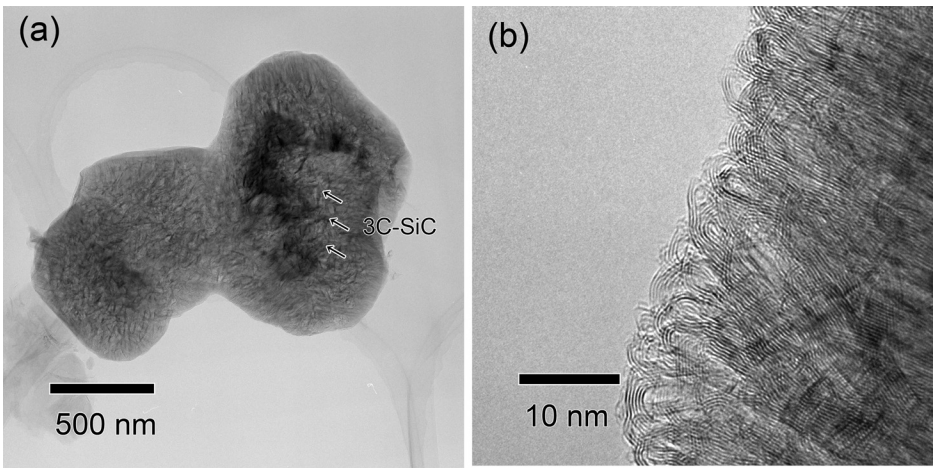

FIG. 4. (a) Low-magnification TEM image of an aggregated CNTs particle. Central dark contrast (shown by arrows) shows a small amount of 3C-SiC. (b) TEM image of the caps of the radially aligned CNTs around the particle.

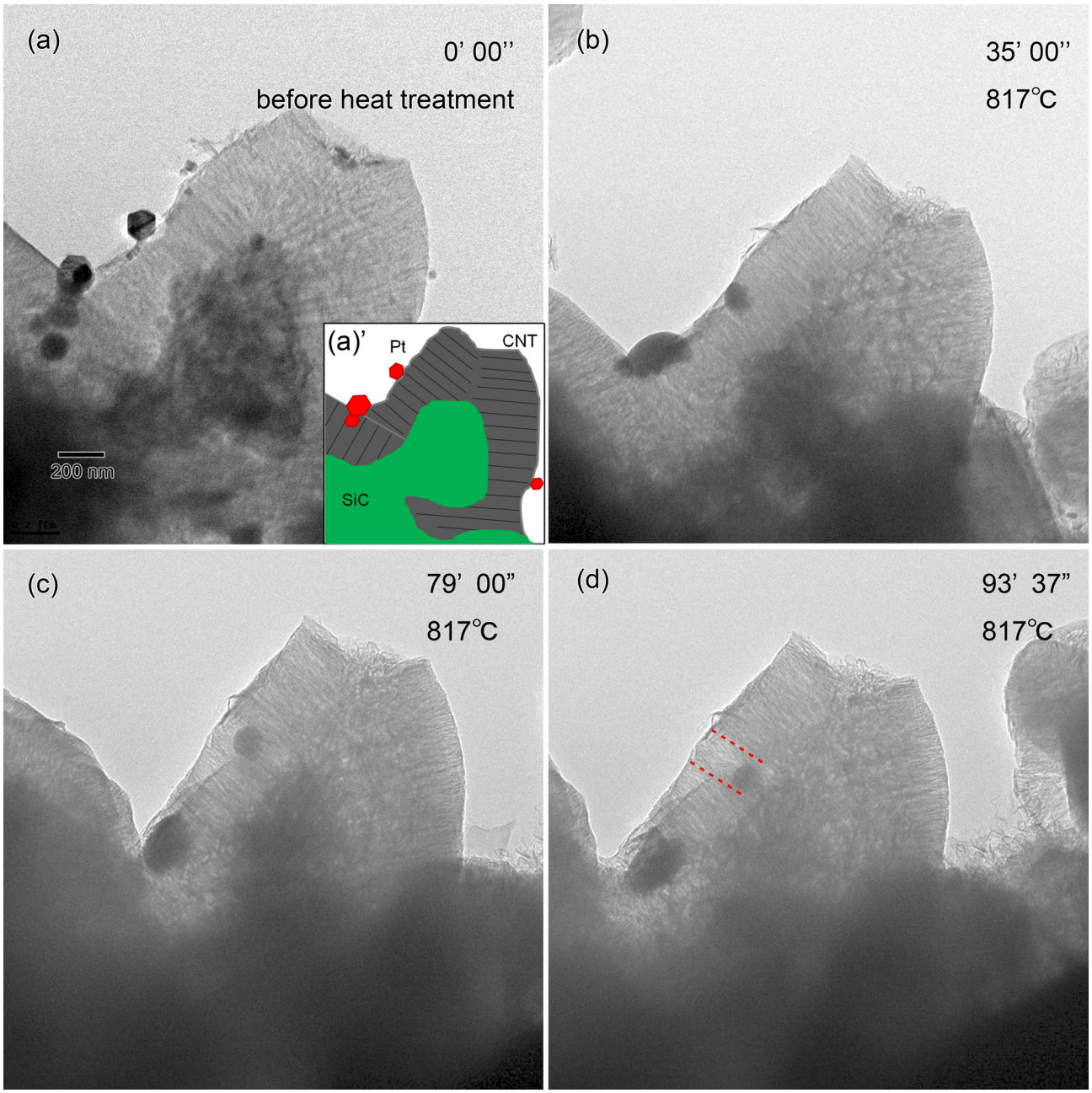

FIG. 5. A series of TEM images during the *in-situ* TEM observation. (a) TEM image of the PtNP on the aggregated CNTs particle before heat treatment and (a)′ schematic diagram in the inset. (b)–(d) Snapshots during heating at 817 °C at 35 min, 79 min, and 94 min, respectively. The video was edited for 60 times speed reproduction. (See supplementary material)

platinum oxides, as was in the sample 2, the PtNPs are mostly reduced in the early stages. The reduced PtNPs then diffuse into the CNTs and coalesce along the CNT walls, forming Pt (111) facets. These results are in very good agreement with a theoretical report, which showed the stable coalescence of Pt nanoclusters with the Pt (111) plane on graphite.[20] In the case of sample 3, the redox reaction did not progress sufficiently for opening of the CNT caps to occur because the amount of platinum oxides was insufficient (the ratio of the oxides was about 20%), which hinders the Pt penetration.

One might think that the electron irradiation during the *in-situ* observation may be another driving force for this behavior. However, first, it was confirmed that the electron irradiation at the high accelerating voltage of 1000 kV at room temperature and at 800 °C did not affect the structure of the aggregated CNT particles. This was surprising because the knock-on threshold voltage of the carbon atom is about only 80 keV.[21] Recently, it was theoretically reported that the position of the carbon atom in the CNT affected the probability of a knock-on process.[22] In our aggregated CNT particles, the CNTs are closely packed and are in contact with each other, which might reduce the knock-on probability, even at a high voltage. Another reason why the electron irradiation did not affect the structure of the CNT particles might be a defect healing. It is known that the CNTs show a self-healing behavior under electron irradiation at moderately high temperature.[23,24] Thus, simultaneous occurrence

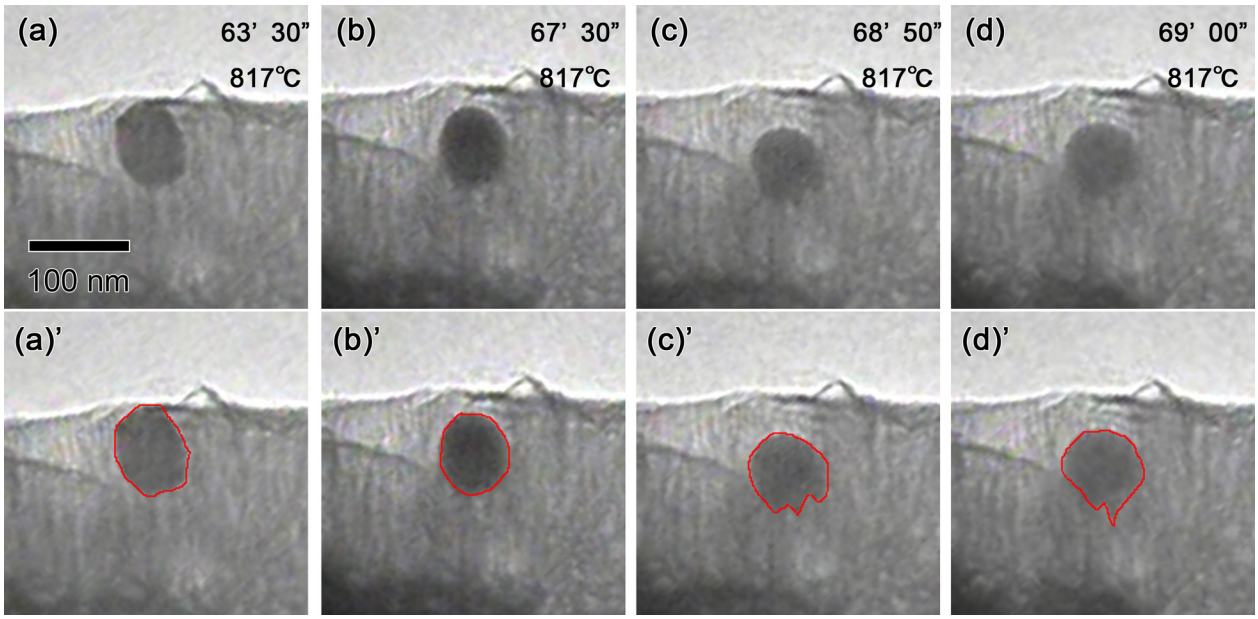

FIG. 6. (a)–(d) A series of TEM images of the PtNP movement observed at elevated temperatures. (a)′–(d)′ We delineated the PtNP, as the image contrast of each image picked up from the movie frames was not clear.

of the knock-on and the defect healings processes might maintain the structure during the *in-situ* observation. Second, the movement of the PtNPs was observed only at high temperatures with oxygen flow. This result indicates that thermal energy and oxygen was primarily necessary for the reaction, supporting the mechanism mentioned above, which might be enhanced by the electron beam irradiation.

We also discuss about the origin of the PtNPs' shape change during the *in-situ* observation. We attribute it to the surface instability during the oxidation and the reduction processes. In our experimental results, the faceted platinum metal became round-shaped platinum oxide just after heating it in oxygen atmosphere, and then it moved into the CNTs. These results indicated that the oxidation and reduction simultaneously and continuously occurred at the interface between the PtNP and the CNT during the *in-situ* observation. Recently, oxidation and reduction of the PtNP's surface were directly observed at atomic-scale by E-TEM.[16] It was revealed there that the surface oxidation proceeded more on the Pt {200} planes than on the Pt {111} planes, while the reduction proceeded on {111} planes rather than on {200} planes. This result suggests that when the oxidation and reduction occurs simultaneously, the surface shape of the PtNP would change continuously. We also showed the tendency that the Pt {111} facet was formed parallel to the CNT wall. These facts can well explain the PtNPs' shape change during the observation.

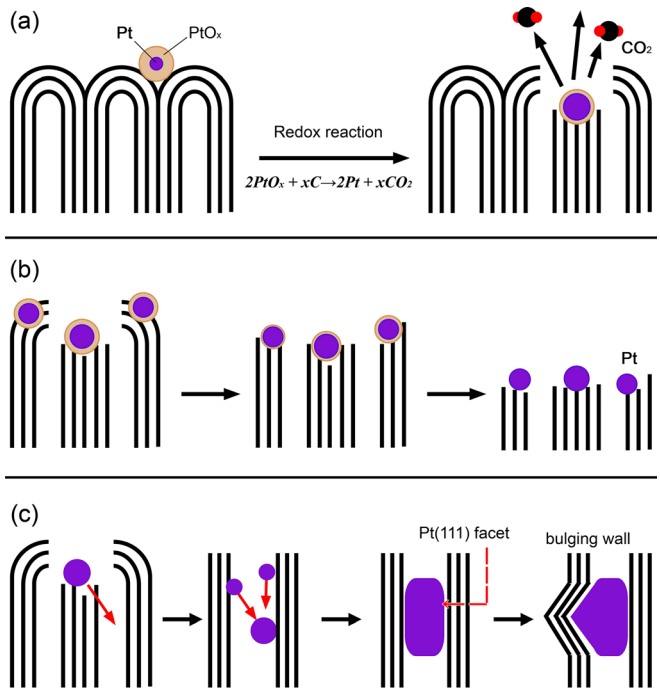

FIG. 7. Schematic diagram of the phenomenon. (a) The redox reaction between the platinum oxides and the CNTs occurs and leads to opening of the CNT caps. (b) In the case of an oxide-rich sample, the redox reaction proceeds. (c) In the case of a metal-rich sample, the oxides are reduced at an early stage. The reduced-PtNPs diffuse in the CNTs and grow up at a point along the CNT walls.

V. CONCLUSION

We have elucidated a key factor in the phenomenon that the Pt deposited on the CNT films etches the CNTs at high temperature in air. We consider that the phenomenon originates with the redox reaction between the platinum oxides and the CNTs. At elevated temperatures, only carbon atoms of the CNTs contacting just in the vicinity of the PtNPs will be able to act effectively as a reducing agent. And then, the redox reaction will progress. The PtNPs are reduced, diffuse into the CNTs, and coalesce. We could also observe the dynamic behavior of the PtNP at elevated temperatures with oxygen gas flow using E-TEM. The PtNP tunnels down into the CNTs along the axis with extending "tentacles," as if desiring carbon atoms. The driving force of the behavior was the redox reaction at a high temperature under the oxygen flow.

SUPPLEMENTARY MATERIAL

See supplementary material for the *in*-situ TEM observation. A part of this work was supported by JSPS KAKENHI Grant Number 25107002; Microstructure Analysis Platform in Nanotechnology Platform Project of the Ministry of Education, Culture, Sports, Science and Technology (MEXT), Japan; and Program for Leading Graduate Schools "Integrative Graduate Education and Research in Green Natural Sciences," MEXT, Japan.

[1]S. Iijima, Nature **354**, 56 (1991).
[2]M. Kusunoki, T. Suzuki, T. Hirayama, and N. Shibata, Appl. Phys. Lett. **77**, 531 (2000).
[3]M. Kusunoki, C. Honjo, T. Suzuki, and T. Hirayama, Appl. Phys. Lett. **87**, 103105 (2005).
[4]M. Kusunoki, T. Suzuki, K. Kaneko, and M. Ito, Philos. Mag. Lett. **79**, 153 (1999).
[5]W. Li, C. Liang, W. Zhou, J. Qiu, Z. Zhou, G. Sun, and Q. Xin, J. Phys. Chem. B **107**, 6292 (2003).
[6]P. J. Britto, K. S. V. Santhanam, A. Rubio, J. A. Alonso, and P. M. Ajayan, Adv. Mater. **11**, 154 (1999).
[7]V. Lordi, N. Yao, and J. Wei, Chem. Mater. **13**, 733 (2001).
[8]M. A. Fraga, E. Jordão, M. J. Medes, M. M. Freitas, J. L. Faria, and J. L. Figueiredo, J. Catal. **209**, 355 (2002).
[9]X. Sun, R. Li, D. Villers, J. P. Dodelet, and S. Désilets, Chem. Phys. Lett. **379**, 99 (2003).
[10]Y. Mu, H. Liang, J. Hu, L. Jiang, and L. Wan, J. Phys. Chem. B **109**, 22212 (2005).
[11]R. H. Baughman, A. A. Zakhidov, and W. A. de Heer, Science **297**, 787 (2002).
[12]T. W. Ebbesen, H. J. Lezec, H. Hiura, J. W. Bennett, H. F. Ghaemi, and T. Thio, Nature **382**, 54 (1996).
[13]J. Wang, G. Yin, Y. Shao, Z. Wang, and Y. Gao, J. Phys. Chem. C **112**, 5784 (2008).
[14]K. Matsuda, W. Norimatsu, and M. Kusunoki, e-J. Surf. Sci. Nanotechnol. **10**, 198 (2012).
[15]N. Tanaka, J. Usukura, M. Kusunoki, Y. Saito, K. Sasaki, T. Tanji, S. Muro, and S. Arai, Kenbikyo **46**, 156 (2011) (in Japanese).
[16]H. Yoshida, H. Omote, and S. Takeda, Nanoscale **6**, 13113 (2014).
[17]G. M. Bancroft, I. Adams, L. L. Coatsworth, C. D. Bennewitz, J. D. Brown, and W. D. Westwood, Anal. Chem. **47**, 586 (1975).
[18]M. Kusonoki, T. Suzuki, C. Honjo, H. Usami, and H. Kato, J. Phys. D: Appl. Phys. **40**, 6278 (2007).
[19]*The Oxide Handbook*, edited by G. V. Samsonov (IFI/Plenum, New York, 1973).
[20]S. H. Lee, S. S. Han, J. K. Kang, J. H. Ryu, and H. M. Lee, Surf. Sci. **602**, 1433 (2008).
[21]B. W. Smith and D. E. Luzzi, J. Appl. Phys. **90**, 3509 (2001).
[22]A. Zobelli, A. Gloter, C. P. Ewels, G. Seifert, and C. Colliex, Phys. Rev. B **75**, 245402 (2007).
[23]A. Kis, K. Jensen, S. Aloni, W. Mickelson, and A. Zettl, Phys. Rev. Lett. **97**, 025501 (2006).
[24]A. V. Krasheninnikov and F. Banhart, Nat. Mater. **6**, 723 (2007).